Tunable shot noise in parallel-coupled double quantum dots' system

2008 J. Phys.: Condens. Matter 20 365206

(http://iopscience.iop.org/0953-8984/20/36/365206)

IOP PUBLISHING JOURNAL OF PHYSICS: CONDENSED MATTER

J. Phys.: Condens. Matter **20** (2008) 365206 (10pp) doi:10.1088/0953-8984/20/36/365206

Tunable shot noise in parallel-coupled double quantum dots' system

Ling Qin and Yong Guo[1]

Department of Physics and Key Laboratory of Atomic and Molecular NanoSciences, Ministry of Education, Tsinghua University, Beijing 100084, People's Republic of China

E-mail: guoy66@tsinghua.edu.cn

Received 15 April 2008, in final form 9 July 2008
Published 14 August 2008
Online at stacks.iop.org/JPhysCM/20/365206

Abstract

We investigate the current and the shot noise in a system composed of two quantum dots symmetrically connected to two external leads. Within the technique of quantum rate equations, the general expressions for the current and the shot noise are derived. It is found that, when the energy levels of the two dots are not aligned, the interdot coupling can result in super-Poissonian shot noise. By tuning the external magnetic flux symmetrically applied to the system, the transition between sub-Poissonian and super-Poissonian noise can be realized. If the distribution of the magnetic flux is inhomogeneous, the shot noise can be reduced or further enhanced.

1. Introduction

In mesoscopic systems, owing to the discrete nature of electrons, the current is fluctuating in time even under dc bias. This fluctuation is called the shot noise, which is a nonequilibrium property of the system in the sense that it is nonzero only when there is a finite current. It characterizes the temporal correlations between individual electron transfers through mesoscopic systems and thus contains additional information about the transport not contained in the average current [1, 2]. In recent years, the shot noise has received increased attention, since it has been proved to be a useful tool to study the role of electron coherence and Coulomb interaction in electron transport [3], which is one of the main subjects in mesoscopic physics. The experimental measurements of shot noise have already been performed in many kinds of systems, such as superconductor [4, 5], fractional Hall liquid [6, 7], quantum dot systems [8, 9], etc.

Totally uncorrelated current results in the so-called full or Poissonian shot noise [10]. The transfer of electrons can be described by Poisson statistics, and the low-frequency noise power is $S = 2eI$, where e is the electron charge and I is the average current. If additional sources of correlations between two consecutive electron transfers are presented, the shot noise can be enhanced or suppressed from its Poisson value. So it is convenient to characterize the correlations by the Fano factor $F = S/2eI$, which is larger (smaller) than unity when positive (negative) correlations exist. In most mesoscopic systems, sub-Poissonian shot noise is observed. The negative correlations may be exerted by Pauli exclusion, which limits the density of electrons in phase space, or by Coulomb repulsion. Both of the two are predicted to impose a time delay between two consecutive electron transfers and suppress the noise [11, 12]. For example, in symmetrical double-barrier junctions the shot noise is reduced to $F = 1/2$ [13, 14]. However, in certain situations the Coulomb repulsion can also yield a positive correlation and enhance the noise even to be super-Poissonian. This phenomenon was first discovered in double-barrier tunneling diode in the negative differential conductance (NDC) regime [15–18] and a Fano factor up to 6.6 was observed. In the NDC regime, the energy of the confined state in the well falls below the conduction band of the electrode. When an electron tunnels into the well, the potential energy of the well is raised. As a consequence, the density of states in the well is shifted upwards, and more states are available for electron tunneling. Therefore, electrons entering the well are positively correlated and the shot noise is enhanced. Recently, it has been predicted that the super-Poissonian noise can also be observed in quantum dot (QDs) systems [19–25]. In a system composed of a two-level QD (or two QDs) coupled to external electrodes, super-Poissonian noise can occur if the two energy levels have different coupling strengths to the leads (for example, QD coupled to ferromagnetic leads [24, 25]). This is because the electrons are harder to tunnel out of the level with weaker coupling strength, and the currents are mainly

[1] Author to whom any correspondence should be addressed.

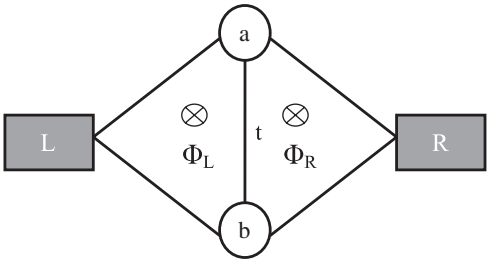

Figure 1. The system with two quantum dots coupled to two external leads. The interdot coupling divides the system into two parts. An external magnetic field threads the system and the magnetic flux enclosed in the left (right) part of the system is denoted by Φ_L (Φ_R).

contributed by the transport through the strongly coupled level. Owing to the large Coulomb repulsion, the occupation of the weakly coupled level can modulate the current through the strongly coupled level. Once it is occupied, transport through the strongly coupled level is blocked and the total current is suppressed. While it is empty, the current can flow through the strongly coupled level. Therefore, the tunneling events are bunched within the time interval when the weakly coupled level is empty and the current fluctuation is enhanced. This is the so-called dynamical channel blockade, which is the crucial ingredient to observe super-Poissonian noise in QD systems. Meanwhile, theoretical works pointed out that super-Poissonian noise can also be observed in symmetrical QD systems [26–28]. For example, two-quasiparticle scattering results in a Fano factor up to 5/3 in the Kondo regime [26]. In a two-level QD system, the shot noise can be tuned back and forth between sub- and super-Poissonian character by using an ac driving field [27].

In the present work we propose a different scheme to generate super-Poissonian noise in a symmetrical QD system. Furthermore, the value of the shot noise can be easily and accurately controlled. The structure is sketched in figure 1, where two quantum dots a and b are embedded in an Aharonov–Bohm interferometer, which is threaded by a magnetic flux. Such a kind of structure has already been realized in experiments [29, 30], where the interdot coupling can be continuously tuned in a wide range and the electron's phase coherence can be sustained. In the present work only one energy level in each dot is assumed to be relevant and the interdot Coulomb repulsion is considered. We will show that, even if the two QDs are symmetrically coupled to the leads, super-Poissonian noise can also be generated in such a system, provided that the interdot coupling is taken into account. Besides, by tuning the magnetic flux we can realize the transition between super- and sub-Poissonian noise. Finally, the effects of the interdot coupling in the asymmetrical system is also studied and we find that, in different transport regimes, the interdot coupling has quite different effects on the shot noise.

The rest of this paper is organized as follows. In section 2, we give the system Hamiltonian and derivations of the expression for the shot noise within the quantum rate equations. Numerical calculations and discussions are presented in section 3 and conclusions are given in section 4.

2. Theoretical framework

We model the system with the Hamiltonian $H = H_{\rm dot} + H_{\rm lead} + H_{\rm T}$. Here $H_{\rm lead} = \sum_{k,\alpha=L,R} \epsilon_{k\alpha} a^\dagger_{k\alpha} a_{k\alpha}$ describes the two noninteracting leads, where $a^\dagger_{k\alpha}$ ($a_{k\alpha}$) is the creation (annihilation) operator for electrons in lead α with wavevector k. The double QDs are described by $H_{\rm dot} = \epsilon_a d^\dagger_a d_a + \epsilon_b d^\dagger_b d_b - t{\rm e}^{{\rm i}\theta/2} d^\dagger_a d_b - t{\rm e}^{-{\rm i}\theta/2} d^\dagger_b d_a + U d^\dagger_a d_a d^\dagger_b d_b$ and the tunneling Hamiltonian between dots and leads is $H_{\rm T} = \sum_{k,\alpha}(V^\alpha_a d^\dagger_a a_{k\alpha} + V^\alpha_b d^\dagger_b a_{k\alpha}) + {\rm H.c.}$ [31–33], where $V^L_a = |V^L_a|{\rm e}^{{\rm i}\phi/4}$, $V^L_b = |V^L_b|{\rm e}^{-{\rm i}\phi/4}$, $V^R_a = |V^R_a|{\rm e}^{-{\rm i}\phi/4}$ and $V^R_b = |V^R_b|{\rm e}^{{\rm i}\phi/4}$. For simplicity, $V^\alpha_{a,b}$ are assumed to be independent of k, and in the symmetrical system we further assume $|V^L_a| = |V^L_b| = |V^R_a| = |V^R_b| = V$. Here we have chosen the symmetric gauge with $\phi = 2\pi(\Phi_L + \Phi_R)/\Phi_0$, where Φ_0 is the flux quantum and $\Phi_{L,R}$ are the magnetic flux penetrating the left and the right parts of the structure, respectively. $\theta = 2\pi(\Phi_R - \Phi_L)/\Phi_0$ describes the magnetic flux imbalance. $\epsilon_{a,b}$ are the energy levels of the two dots, U is the interdot Coulomb repulsion strength, t is the interdot coupling strength and $d^\dagger_{a,b}$ ($d_{a,b}$) are the creation (annihilation) operators for electrons in dots a and b. The intradot Coulomb repulsion is assumed to be strong enough that the double occupation of each dot is forbidden and the spin degree of freedom is ignored here.

In this work we focus on the regime where the temperature $k_{\rm B}T$ is much smaller than the Coulomb repulsion strength U and the dot–lead coupling strength $\Gamma = 2\pi \sum_k |V|^2 \delta(\epsilon - \epsilon_{k\alpha})$ is much weaker than $k_{\rm B}T$. In the following, we adopt the method used by Djuric *et al* [25] to derive the expressions for the current and the shot noise with the aid of quantum rate equations. In [25] the authors have studied the transport properties of a system composed of a QD coupled to ferromagnetic leads. It is clear that the spin-degenerate level and the spin-flip process in their work play similar roles to the two QD levels and the interdot coupling in our work, respectively. However, the authors directly performed the quantum rate equations, and the spin-flip process was taken into account by the nondiagonal elements of the density matrix. Such a technique is only valid when the spin-flip scattering is weak [25, 34], so the level splitting induced by the spin-flip scattering is absent in their work and the zero-frequency current fluctuation is suppressed by the spin-flip scattering. In our work, to completely take into account the effects of the interdot coupling, we first make a unitary transformation to diagonalize the Hamiltonian before carrying out the quantum rate equations. Now the interdot coupling t is absorbed into the energies of the bonding and antibonding states, and can be of arbitrary value. Thus, the level splitting takes place and we find the interdot coupling can even enhance the shot noise. The transformation is performed as

$$\begin{pmatrix} d_1 \\ d_2 \end{pmatrix} = \begin{pmatrix} \cos\beta {\rm e}^{-{\rm i}\theta/2} & -\sin\beta \\ \sin\beta & \cos\beta {\rm e}^{{\rm i}\theta/2} \end{pmatrix} \begin{pmatrix} d_a \\ d_b \end{pmatrix},$$

where $\beta = \frac{1}{2}\arctan(2t/\delta\epsilon)$ with $\delta\epsilon = \epsilon_a - \epsilon_b$ (we assume $\epsilon_a \geqslant \epsilon_b$). Then $H_{\rm dot}$ reduces to $H_{\rm dot} = \epsilon_1 d^\dagger_1 d_1 + \epsilon_2 d^\dagger_2 d_2 + U d^\dagger_1 d_1 d^\dagger_2 d_2$, where $\epsilon_1 = \bar{\epsilon} + (t^2 + \delta\epsilon^2/4)^{1/2}$ and $\epsilon_2 = \bar{\epsilon} - (t^2 + \delta\epsilon^2/4)^{1/2}$ are the energies of the so-called antibonding and bonding states, respectively. Here

$\bar{\epsilon} = (\epsilon_a + \epsilon_b)/2$, and $d_1(d_1^\dagger)$ and $d_2(d_2^\dagger)$ are the annihilation (creation) operators for the antibonding and bonding states. Correspondingly, the tunneling Hamiltonian is transformed to $H_T = \sum_{k,\alpha}(V_1^\alpha d_1^\dagger a_{k\alpha} + V_2^\alpha d_2^\dagger a_{k\alpha}) + \text{H.c.}$, where $V_1^L = V[\cos\beta e^{i(\phi-2\theta)/4} - \sin\beta e^{-i\phi/4}]$, $V_2^L = V[\cos\beta e^{i(2\theta-\phi)/4} + \sin\beta e^{i\phi/4}]$, $V_1^R = V[\cos\beta e^{-i(\phi+2\theta)/4} - \sin\beta e^{i\phi/4}]$, and $V_2^R = V[\cos\beta e^{i(\phi+2\theta)/4} + \sin\beta e^{-i\phi/4}]$.

Following the procedure developed by Dong *et al* [34], we can describe the electronic transport by the quantum rate equations $d\rho/dt = \mathbf{M}\rho$, where $\rho = (\rho_{00}, \rho_{11}, \rho_{22}, \rho_{dd})^T$ and

$$\mathbf{M} = \begin{pmatrix} -\Gamma_1^+ - \Gamma_2^+ & \Gamma_1^- & \Gamma_2^- & 0 \\ \Gamma_1^+ & -\widetilde{\Gamma}_2^+ - \Gamma_1^- & 0 & \widetilde{\Gamma}_2^- \\ \Gamma_2^+ & 0 & -\widetilde{\Gamma}_1^+ - \Gamma_2^- & \widetilde{\Gamma}_1^- \\ 0 & \widetilde{\Gamma}_2^+ & \widetilde{\Gamma}_1^+ & -\widetilde{\Gamma}_1^- - \widetilde{\Gamma}_2^- \end{pmatrix}.$$

Here ρ_{00} denotes the probability that the double-dot system is empty, ρ_{11} (ρ_{22}) represents the probability that state 1 (2) is occupied by one electron and ρ_{dd} stands for the double occupation. These four elements of the density matrix satisfy the completeness relation $\rho_{00} + \rho_{11} + \rho_{22} + \rho_{dd} = 1$. $\Gamma_i^\pm = \sum_{\alpha=L,R}\Gamma_i^{\alpha\pm} = \sum_{\alpha=L,R}\Gamma_i^\alpha f_\alpha^\pm(\epsilon_i)$ and $\widetilde{\Gamma}_i^\pm = \sum_{\alpha=L,R}\widetilde{\Gamma}_i^{\alpha\pm} = \sum_{\alpha=L,R}\Gamma_i^\alpha f_\alpha^\pm(\epsilon_i + U)$ $(i = 1, 2)$, where $f_\alpha^+(\omega) = f_\alpha(\omega)$ and $f_\alpha^-(\omega) = 1 - f_\alpha(\omega)$. $f_\alpha(\omega) = [1 + e^{(\omega-\mu_\alpha)/k_BT}]^{-1}$ is the Fermi distribution function of lead α, where μ_α is the Fermi level. Here we take the equilibrium Fermi level as the energy reference and assume the bias is symmetrically applied between source and drain, i.e. $\mu_L = -\mu_R = eV/2$. $\Gamma_i^\alpha = 2\pi\sum_k |V_i^\alpha|^2\delta(\epsilon - \epsilon_{k\alpha})$ are the effective coupling strengths between lead α and state i, and can be explicitly expressed as $\Gamma_1^L = \Gamma(1 - \sin 2\beta\cos\frac{\phi-\theta}{2})$, $\Gamma_2^L = \Gamma(1 + \sin 2\beta\cos\frac{\phi-\theta}{2})$, $\Gamma_1^R = \Gamma(1 - \sin 2\beta\cos\frac{\phi+\theta}{2})$ and $\Gamma_2^R = \Gamma(1 + \sin 2\beta\cos\frac{\phi+\theta}{2})$. Clearly they satisfy the relation $\Gamma_1^\alpha + \Gamma_2^\alpha = 2\Gamma$. The steady state solution of the density matrix can be solved from $\mathbf{M}\rho^{(0)} = 0$ and the current through lead α is $I_\alpha = e/h\sum_n[\hat{\Gamma}_\alpha\rho^{(0)}]_n$, where

$$\hat{\Gamma}_\alpha = \pm\begin{pmatrix} 0 & -\Gamma_1^{\alpha-} & -\Gamma_2^{\alpha-} & 0 \\ \Gamma_1^{\alpha+} & 0 & 0 & -\widetilde{\Gamma}_2^{\alpha-} \\ \Gamma_2^{\alpha+} & 0 & 0 & -\widetilde{\Gamma}_1^{\alpha-} \\ 0 & \widetilde{\Gamma}_2^{\alpha+} & \widetilde{\Gamma}_1^{\alpha-} & 0 \end{pmatrix}.$$

Here $+$ for $\alpha = L$ and $-$ for $\alpha = R$, and $\sum_n[A]_n$ denotes the summation over all vector elements of A ($n = 1, 2, 3, 4$). The current noise spectrum is defined as $S_{\alpha\alpha'}(\omega) = 2\int_{-\infty}^{\infty} dt e^{i\omega t}[\langle I_\alpha(t)I_{\alpha'}(0)\rangle - \langle I_\alpha\rangle\langle I_{\alpha'}\rangle]$. To express it by the system parameters we need to perform the spectral decomposition of $\mathbf{M}$: $\mathbf{M} = \sum_n \lambda_n S E^{(nn)} S^{-1} = \sum_\lambda \lambda P_\lambda$, where λ_n are the eigenvalues of $\mathbf{M}$ and $E^{(nn)}$ is a 4×4 matrix with the (n, n) element 1 and all other elements zero. Since $\det(\mathbf{M}) = 0$, there will always be an eigenvalue $\lambda_1 = 0$. After the decomposition, the zero-frequency noise spectrum is expressed as

$$S_{\alpha\alpha'}(0) = \delta_{\alpha\alpha'}S^{\text{Sch}} - 2e^2/h \times \sum_{n,\lambda\neq 0}\left(\frac{[\hat{\Gamma}_\alpha P_\lambda\hat{\Gamma}_{\alpha'}\rho^{(0)} + \hat{\Gamma}_{\alpha'}P_\lambda\hat{\Gamma}_\alpha\rho^{(0)}]_n}{\lambda}\right), \quad (1)$$

where $S^{\text{Sch}} = 2eI$ is the frequency-independent Schottky noise.

3. Numerical results and discussions

For numerical calculations, we choose meV to be the energy unit and set $k_BT = 0.05$. The currents are normalized to $e\Gamma/h$. First, we do not take into account the effect of the magnetic flux. Now we have $\Gamma_i^L = \Gamma_i^R$ and, for convenience, we denote Γ_i^α by Γ_i with $\Gamma_1 = \Gamma(1 - \sin 2\beta)$ and $\Gamma_2 = \Gamma(1 + \sin 2\beta)$. In figures 2(a) and (b) we show the variations of the current and the Fano factor with the bias voltage in four different situations: (a) $t = \delta\epsilon = 0$, (b) $t = 0$, $\delta\epsilon \neq 0$, (c) $t \neq 0$, $\delta\epsilon \neq 0$ and (d) $t \neq 0$, $\delta\epsilon = 0$. The Coulomb repulsion U is chosen to be larger than $\epsilon_1 - \epsilon_2$. In case (a) the system reduces to a symmetrical structure with two degenerate levels, and in the I–V curve there are two steps locating at ϵ_a and $\epsilon_a + U$. In the zero bias limit, the noise is dominated by the thermal noise and divergent. With the voltage increasing, the shot noise dominates and the Fano factor reduces to unity before the Fermi level of the left lead μ_L reaches the resonant level ϵ_a, because in this region the transport is thermally activated and the tunneling events are uncorrelated. When the resonant level enters the bias window, the Fano factor reduces to 5/9 [20, 35] and equals 1/2 when $\mu_L > \epsilon_a + U$. In case (b) the whole bias range is divided into four regions, and the current and the Fano factor keep constant values in every region. Now the current increases monotonically with the bias, while the Fano factor depends non-monotonically on the bias and is always smaller than unity [35]. In case (c) there are also four transport regions. Now we have $0 < \beta < \pi/4$ and $\Gamma_1 \ll \Gamma_2$, so the electrons in the antibonding state can block the tunneling through the bonding state before the Coulomb repulsion is overcome. Thus, the current shows a negative differential structure and the Fano factor is enhanced (later we will discuss the formation of the NDC in detail). Finally, we turn to the special case (d). In this case $\beta = \pi/4$, so we have $\Gamma_1 = 0$ and $\Gamma_2 = 2\Gamma$, i.e. the antibonding state is completely decoupled from the system. This leads to the 'ghost Fano resonance' in the linear conductance spectrum [31, 33, 36, 37], and the system is equivalent to a noninteracting single-level system with $\epsilon_2 = \epsilon_a - t$ and $\Gamma_2 = 2\Gamma$. This situation is trivial, so in the rest of this work we always assume $\delta\epsilon \neq 0$ (although the antibonding state can participate in transport again when the magnetic flux is presented, it will give nothing new from the case that $\delta\epsilon \neq 0$).

Next we carefully study the effect of the interdot coupling on the current and the shot noise. There are four transport regions: $\epsilon_2 < \mu_L < \epsilon_1$, $\epsilon_1 < \mu_L < \epsilon_2 + U$, $\epsilon_2 + U < \mu_L < \epsilon_1 + U$ and $\mu_L > \epsilon_1 + U$, and we denote them by $i = 1, 2, 3, 4$, respectively, which is shown in figure 2(c). We keep ϵ_1 and ϵ_2 to be positive, so μ_R is below all the energy levels. With $t/\delta\epsilon$ increasing, Γ_2 increases and Γ_1 decreases, and the current increases monotonically in regions 1 and 3, since in both regions the current is mainly contributed by the transport through the bonding state. We can also see the shift of the energies of the bonding and antibonding states, which results in the shrinking of region 2 and the expansion of both regions 1 and 3. For a large enough $t/\delta\epsilon$, the current no longer increases monotonically with the bias and the NDC appears when the bias enters region 2, which stems from the partial

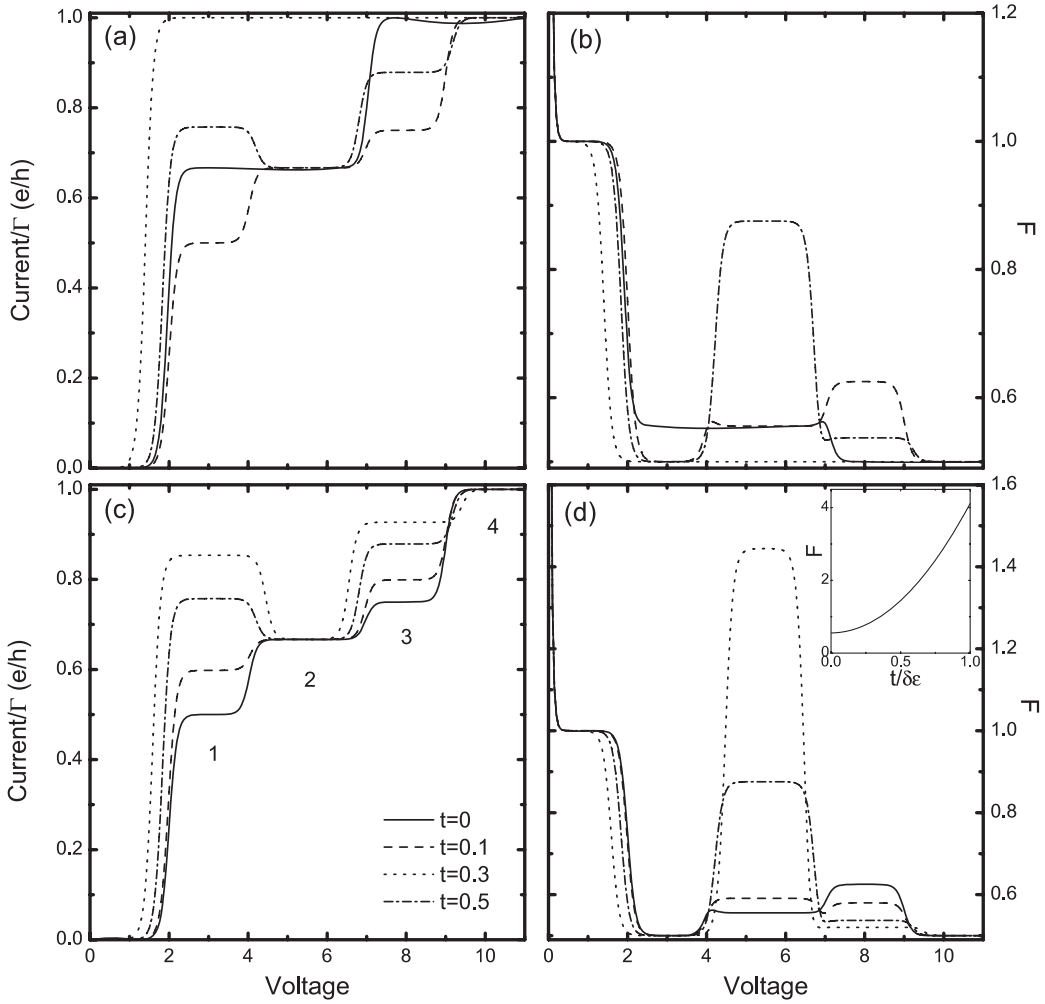

Figure 2. The current and Fano factor versus bias. In (a) and (b) the solid, dashed, dashed–dotted and dotted lines correspond to the cases (a) $t = \delta\epsilon = 0$, (b) $t = 0$, $\delta\epsilon = 1$, (c) $t = 0.3$, $\delta\epsilon = 1$ and (d) $t = 0.3$, $\delta\epsilon = 0$, respectively. In (c) and (d) we assume $\epsilon_a = 1$ and $\epsilon_b = 2$, and the four lines correspond to $t = 0$, 0.1, 0.3 and 0.5, respectively. In the inset we show the Fano factor as a function of $t/\delta\epsilon$ at bias voltage $eV = 5.5$. $U = 2.5$ is assumed in all figures.

blockade of the first electronic channel (bonding state) by the second one (antibonding state) [20, 22]: since now $\Gamma_1 \ll \Gamma_2$, when the second channel opens, the electrons have much longer dwell time in the antibonding state than in the bonding state. If the antibonding state is occupied, transport through the bonding state is quenched, for the simultaneous occupation of both states is energetically forbidden in the considered bias range. Consequently, the transport through the antibonding state modulates the transport through the bonding state and leads to the NDC at $\mu_L = \epsilon_1$. In region 3 the Coulomb repulsion is overcome by the bias voltage and the transport through the bonding state is no longer blocked, so the current increases with the bias again. Different from the current, the Fano factor keeps a constant value 0.5 in regions 1 and 4, because in both regions the transport properties of the system resemble those of a symmetrical noninteracting system. In region 2, the Fano factor increases with $t/\delta\epsilon$ increasing, and finally becomes super-Poissonian, which is explicitly shown in the inset. Thus, the super-Poissonian noise can also be generated in a symmetrical structure, if the energy levels of the two dots are mismatched and the interdot coupling is strong enough. In this case the NDC and the super-Poissonian noise are both generated by dynamical channel blockade, and have been studied in several previous works [20, 22]. However, the NDC and the super-Poissonian noise do not always appear together, as we will see below. Here the occupation of the antibonding state can modulate the current through the bonding state and leads to an effective bunching of tunneling events and, consequently, to the super-Poissonian shot noise. With $t/\delta\epsilon$ increasing, Γ_1/Γ_2 decreases and the bunching gets stronger, so the Fano factor increases. In region 3 the shot noise is always sub-Poissonian, since now the tunneling via the bonding state is no longer blocked.

Now we investigate the effect of the magnetic field. Two situations are considered here: the distribution of the magnetic flux is homogeneous or inhomogeneous. In the first case we have $\phi_L = \phi_R$ (or $\theta = 0$), so $\Gamma_i^L = \Gamma_i^R$ still holds. We also denote Γ_i^α by Γ_i with $\Gamma_1 = \Gamma(1 - \sin 2\beta \cos\frac{\phi}{2})$ and $\Gamma_2 = \Gamma(1 + \sin 2\beta \cos\frac{\phi}{2})$. Since the effective coupling strengths are magnetic-flux-dependent, we expect the transition between super- and sub-Poissonian noise can be realized by tuning the

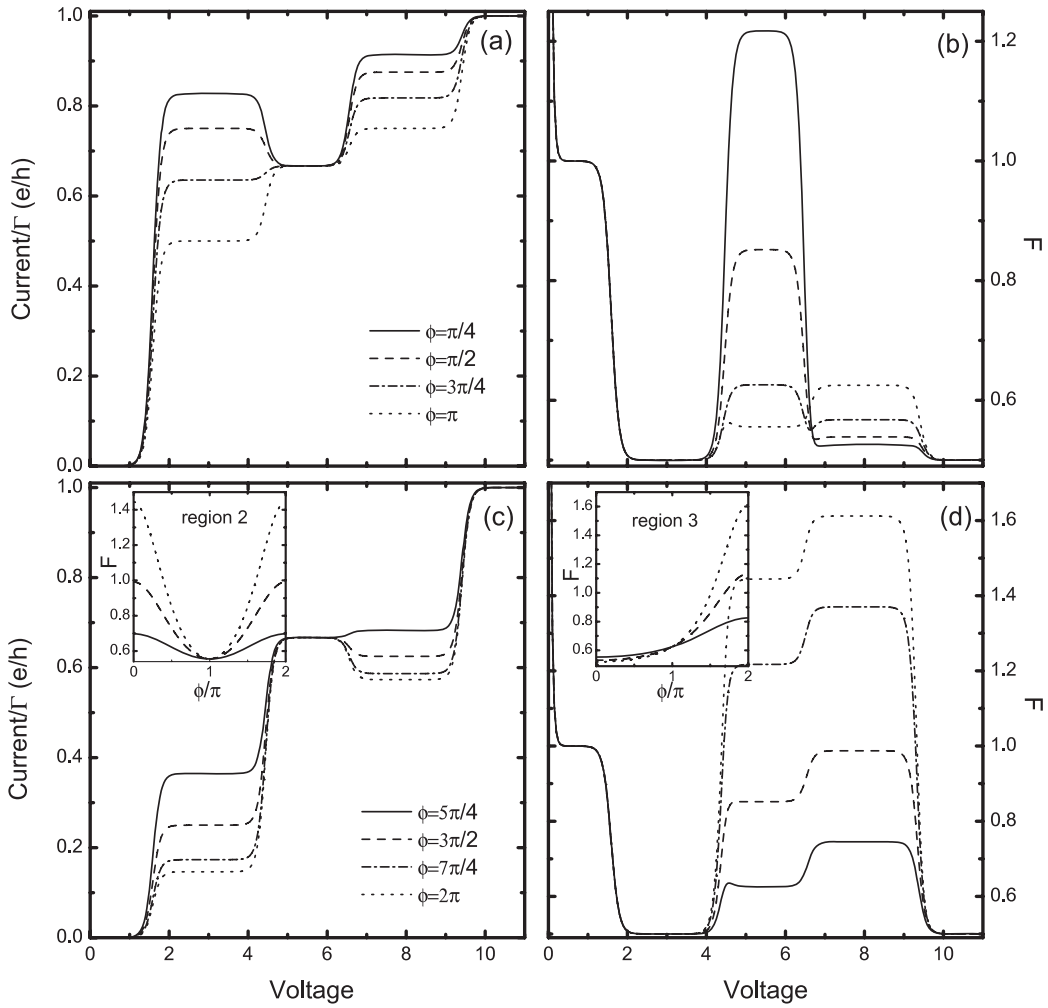

Figure 3. The current and the Fano factor versus bias. In (a) and (b) the solid, dashed, dashed–dotted and dotted lines correspond to $\phi = \pi/4$, $\pi/2$, $3\pi/4$ and π, while in (c) and (d) they correspond to $\phi = 5\pi/4$, $3\pi/2$, $7\pi/4$ and 2π, respectively. $\epsilon_a = 1$, $\epsilon_b = 2$, $t = 0.5$ and $U = 2.5$ are assumed in all figures. In the insets of (c) and (d) we show the ϕ dependence of the Fano factor in regions 2 and 3, where the solid, dashed and dotted lines correspond to $t = 0.2$, 0.35 and 0.5, respectively.

magnetic flux. Figure 3 shows the variations of the current and the Fano factor with bias voltage for different ϕ. To see it clearly, in figures 3(a) and (b) we plot the case for $0 < \phi \leqslant \pi$ and in figures 3(c) and (d) $\pi < \phi \leqslant 2\pi$. When ϕ is small, Γ_1 is much smaller than Γ_2 (according to our parameters, $\sin 2\beta \approx 0.707$, and $\Gamma_1/\Gamma_2 \approx 0.172$ for $\phi = 0$), thus we again obtain the NDC at the bias voltage $\mu_L = \epsilon_1$ and the super-Poissonian noise in region 2. As ϕ increases from 0 to π, Γ_1/Γ_2 increases to 1. Since the transport properties mainly depend on the ratio Γ_1/Γ_2, the features of figures 3(a) and (b) are similar to figures 2(c) and (d) except for the absence of the shift of energy levels, and we do not discuss them anymore. When $\pi < \phi \leqslant 2\pi$, Γ_1 is larger than Γ_2. With ϕ increasing, the current in regions 1 and 3 keeps decreasing, and the NDC transfers from $\mu_L = \epsilon_1$ to $\epsilon_2 + U$. This is because in region 3 a new transport channel at $\epsilon_2 + U$ opens, which increases the possibility that electrons reside in the bonding state. Thus, the transport through the antibonding state is further blocked and the current is suppressed. Therefore, we expect super-Poissonian noise can also appear in region 3. This can be seen in figure 3(d), where the behaviors of the Fano factor are much different from the case when $0 < \phi \leqslant \pi$. Now both in regions 2 and 3 the Fano factor increases with ϕ and its value is even higher in region 3 than that in region 2. Thus, the super-Poissonian noise can be first observed in region 3, which means that we can tune the magnetic flux to change the bias range where the super-Poissonian noise appears (from region 2 to region 3). We also note that there is no NDC when the bias enters region 2 for $\phi > \pi$, while super-Poissonian noise can still happen in region 2 when ϕ approaches 2π. This can be understood as follows. In this region the dynamical channel blockade exists (the bonding state is the weakly coupled state while the antibonding state is the strongly coupled one), so the super-Poissonian noise appears. However, since the bonding state opens first, when the antibonding state opens in region 2, the current keeps increasing and no NDC appears. Thus, we also come to the conclusion that the super-Poissonian noise is related to the dynamical channel blockade rather than the NDC [38, 39].

The behaviors of the Fano factor can be understood as follows. When $\Gamma_1 > \Gamma_2$, in region 2 the case is just the opposite to that when $\Gamma_1 < \Gamma_2$. Now electrons have

longer dwell time in the bonding state, which gives rise to the bunching of tunneling events through the antibonding state. However, in both situations the results are the same: when the discrepancy between Γ_1 and Γ_2 is large enough, super-Poissonian noise appears in this region. The situation is completely different in region 3, where a new channel at $\epsilon_2 + U$ opens and the transport through the bonding state can no longer be blocked. If the bonding state has stronger coupling ($\Gamma_1 < \Gamma_2$), no bunching happens in transport and the shot noise is sub-Poissonian. In contrast, if the antibonding state has stronger coupling ($\Gamma_1 > \Gamma_2$), the electron on the bonding state will result in the bunching of tunneling through the antibonding state and the shot noise can be enhanced to be super-Poissonian. So when $0 < \phi \leqslant \pi$ the super-Poissonian noise only emerges in region 2, while when $\pi < \phi \leqslant 2\pi$ it can emerge in both regions 2 and 3. Besides, owing to the opening of the new tunneling channel, in region 3 electrons have larger probability to reside in the bonding state than that in region 2. As a consequence, the bunching of transport through the antibonding state is further enhanced and the Fano factor is larger than that in region 2 when $\pi < \phi \leqslant 2\pi$. This can be seen more explicitly in the insets in figures 3(c) and (d), where we show the Fano factor as a function of ϕ for several values of $t/\delta\epsilon$ in regions 2 and 3, respectively. As we expect, the Fano factor in region 2 is symmetrical with respect to $\phi = \pi$, while in region 3 it increases monotonically with ϕ. When $\phi > \pi$, in region 3 the Fano factor is always larger than that in region 2. Besides, with $t/\delta\epsilon$ decreasing, the modulation of the Fano factor by the magnetic flux is weakened. When $t/\delta\epsilon$ reduces to a critical value, the shot noise can no longer be enhanced to be super-Poissonian by tuning the magnetic flux. This is because, when $\sin 2\beta$ is small, we cannot obtain a large enough asymmetrical ratio $\Gamma_{1(2)}/\Gamma_{2(1)}$ to induce strong bunching of tunneling events. Thus, the critical value of $t/\delta\epsilon$ is an important parameter and we will evaluate it in the following.

Since the Fano factor is larger in region 3 than that in region 2 for $\phi > \pi$, the critical value of $t/\delta\epsilon$ should be smaller in region 3. To confirm this point, we require the expressions of the physical quantities in every region. Under the conditions $\Gamma_i^L = \Gamma_i^R = \Gamma_i$ and $\Gamma_1 + \Gamma_2 = 2\Gamma$, the eigenvalues of $\mathbf{M}$ are $\lambda_1 = 0$, $\lambda_2 = -4\Gamma$ and $\lambda_{3,4} = -2\Gamma \pm (4\Gamma^2 - \gamma^2)$, where $\gamma = \Gamma_1^+\Gamma_2^- + \Gamma_1^-\Gamma_2^+ + \Gamma_1^-\Gamma_2^- + \widetilde{\Gamma}_1^+\widetilde{\Gamma}_2^+ + \widetilde{\Gamma}_1^+\widetilde{\Gamma}_2^- + \widetilde{\Gamma}_1^-\widetilde{\Gamma}_2^+ - \Gamma_1^-\widetilde{\Gamma}_2^+ - \Gamma_2^-\widetilde{\Gamma}_1^+$. After some algebra we obtain the analytic expressions for the current, the shot noise and the Fano factor in every region, which are given in table 1. For convenience, we define $\chi = \Gamma_1/\Gamma_2$. From the expressions for the current we know that the NDC can happen at $\mu_L = \epsilon_1$ if $\chi < 1/2$, or at $\mu_L = \epsilon_2 + U$ if $\chi > 2$, which has already been revealed in figure 3. To observe super-Poissonian noise in region 2, χ (or $1/\chi$) must be larger than $2+\sqrt{3} \approx 3.73$ and the corresponding $t/\delta\epsilon$ is 0.354, while in region 3 the critical value is $\chi \approx 3.06$ and $t/\delta\epsilon \approx 0.295$. So it is easier to generate super-Poissonian noise in region 3, where a weaker interdot coupling is required. Besides, in region 2 the values of the current and the shot noise remain unchanged with respect to the interchange of Γ_1 and Γ_2. The Fano factor increases monotonically with χ when $\chi > 1$ and diverges when $\chi \to \infty$ or 0. When $\chi = 1$, F reduces to its minimal value 5/9. In region 3, the Fano factor increases monotonically with χ and also diverges when $\chi \to \infty$. When $\chi \to 0$, it reduces to its minimal value 1/2, since now the antibonding state has little effect on the transport and the system resembles a single-level noninteracting system.

Table 1. The analytical results of the current, the shot noise and the Fano factor in different bias regions.

Region	1	2	3	4
$I(e/h)$	$\frac{\Gamma_2}{2}$	$\frac{\Gamma_1+\Gamma_2}{3}$	$\frac{\Gamma_1+2\Gamma_2}{4}$	$\frac{\Gamma_1+\Gamma_2}{2}$
$S(e^2/h)$	$\frac{\Gamma_2}{2}$	$\frac{2(2\Gamma_1^3+3\Gamma_1^2\Gamma_2+3\Gamma_1\Gamma_2^2+2\Gamma_2^3)}{27\Gamma_1\Gamma_2}$	$\frac{\Gamma_1^3+3\Gamma_1^2\Gamma_2+7\Gamma_1\Gamma_2^2+4\Gamma_2^3}{8\Gamma_2(\Gamma_1+\Gamma_2)}$	$\frac{\Gamma_1+\Gamma_2}{2}$
F	$\frac{1}{2}$	$\frac{2\Gamma_1^3+3\Gamma_1^2\Gamma_2+3\Gamma_1\Gamma_2^2+2\Gamma_2^3}{9\Gamma_1\Gamma_2(\Gamma_1+\Gamma_2)}$	$\frac{\Gamma_1^3+3\Gamma_1^2\Gamma_2+7\Gamma_1\Gamma_2^2+4\Gamma_2^3}{4\Gamma_2(\Gamma_1+\Gamma_2)(\Gamma_1+2\Gamma_2)}$	$\frac{1}{2}$

In the above discussions the left–right symmetry of the system is preserved, even when the magnetic field is applied. However, if the distribution of the magnetic flux is inhomogeneous ($\theta \neq 0$), the symmetry is broken, which can be clearly seen from the expressions of Γ_i^α. At this time $\Gamma_i^L \neq \Gamma_i^R$ and the systematical investigation of shot noise in such a kind of completely asymmetrical structure is lacking. Now in regions 1 and 4 the Fano factor does not keep 1/2 anymore [35]. In the following, we focus on the shot noise in region 2 and we can see that the inhomogeneous distribution of the flux has significant influences on the generation and modulation of the super-Poissonian noise. In figure 4(a) we plot the Fano factor in region 2 as a function of ϕ for several values of θ. $t/\delta\epsilon$ is set to be 0.5, which is larger than the critical value in region 2. When $\theta = 0$, the transition between sub- and super-Poissonian noise can be realized by tuning the total magnetic flux. This also holds if θ is small. However, if θ is around π, the shot noise is much more insensitive to the flux and is always sub-Poissonian. This can also be seen in figure 4(c), where we show the Fano factor in region 2 as a function of ϕ and θ for $t/\delta\epsilon = 0.5$ (since the coupling strengths remain unchanged under the interchange of ϕ and θ, this figure is symmetrical with respect to the line $\theta = \phi$). We can understand it as follows. Taking $\theta = \pi$ for example. Then the coupling strengths are $\Gamma_1^L = \Gamma_2^R = \Gamma(1 - \sin 2\beta \sin\frac{\phi}{2})$ and $\Gamma_2^L = \Gamma_1^R = \Gamma(1 + \sin 2\beta \sin\frac{\phi}{2})$. Thus, this situation is similar to that of a QD connected to two ferromagnetic leads with antiparallel aligned magnetizations. In such a structure, the spin-up electrons dominate in the transport and make the noise sub-Poissonian, which has already been studied by Braun *et al* [24]. In our system, the bonding state, which is strongly coupled to the source lead and weakly coupled to the drain lead ($\Gamma_2^L > \Gamma_2^R$), plays the similar role of the spin-up state in their work. Therefore, the shot noise is always sub-Poissonian when θ is about π. To obtain analytical results of the Fano factor, we resort equation (1) once more. Under the condition $\Gamma_2^L = 2\Gamma - \Gamma_1^L$ and $\Gamma_2^R = 2\Gamma - \Gamma_1^R$, we obtain

$$\begin{aligned} F = {} & (\Gamma_1^R)^4 - 4\Gamma(\Gamma_1^R)^3 + (\Gamma_1^R)^2[8\Gamma^2 + 8\Gamma\Gamma_1^L - 4(\Gamma_1^L)^2] \\ & - 8\Gamma_1^R[3\Gamma^2\Gamma_1^L - \Gamma(\Gamma_1^L)^2] + 4\Gamma^2\Gamma_1^L(4\Gamma - \Gamma_1^L) \\ & \times \{[(\Gamma_1^R)^2 - 4\Gamma\Gamma_1^R + 2\Gamma_1^L\Gamma_1^R - 2\Gamma\Gamma_1^L]^2\}^{-1}. \end{aligned} \tag{2}$$

When $\theta = \pi$, we have $\Gamma_1^R = 2\Gamma - \Gamma_1^L$ and $F = [4\Gamma^2 + 2\Gamma\Gamma_1^L - (\Gamma_1^L)^2][4\Gamma^2 - 6\Gamma\Gamma_1^L + 3(\Gamma_1^L)^2]/[4\Gamma^2 - 2\Gamma\Gamma_1^L + (\Gamma_1^L)^2]^2$. It is easy to see that F is always smaller than 1, and approaches 1 when $\Gamma_1^L \to 0$ or 2Γ. So when $\theta = \pi$, we cannot generate

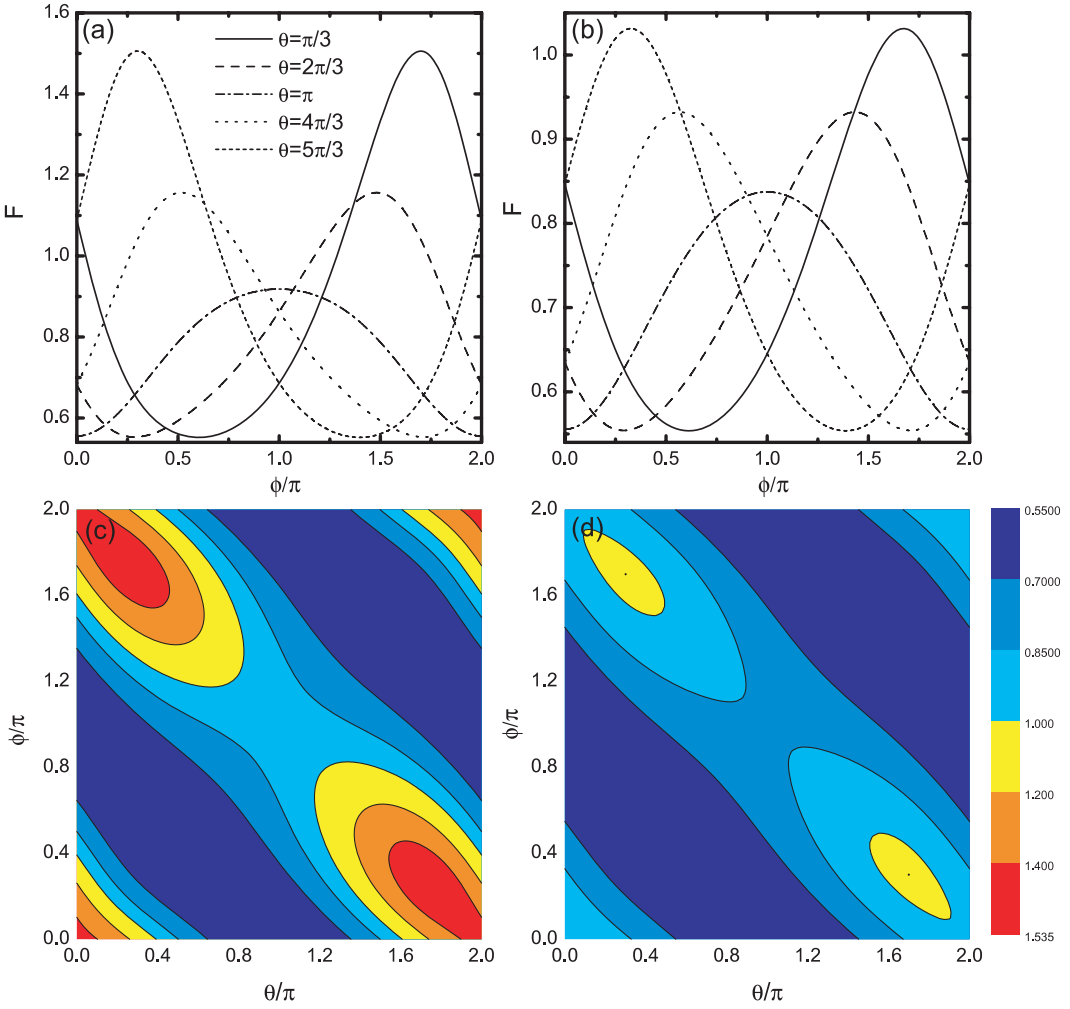

Figure 4. The Fano factor as a function of ϕ for (a) $t/\delta\epsilon = 0.5$ and (b) $t/\delta\epsilon = 0.35$ when the bias is in region 2. In (c) and (d) we show the Fano factor as a function of ϕ and θ for $t/\delta\epsilon = 0.5$ and 0.35, respectively.

(This figure is in colour only in the electronic version)

super-Poissonian noise in the symmetrical system, even if $t/\delta\epsilon$ exceeds the critical value.

In figure 4(a) we can also see that, for a fixed θ, the Fano factor reaches its maximum when $\theta + \phi \approx 2\pi$. We have already known that, when the distribution of the flux is homogeneous, the Fano factor reaches its maximum when $\phi = 2\pi$ (or $\phi = 0$), which can be viewed as a special case for $\theta = 0$. It is displayed more explicitly in figure 4(c) that, around the line $\theta + \phi = 2\pi$, the Fano factor is always larger than that when $\theta = 0$. So the shot noise can be further enhanced when the distribution of the magnetic flux is inhomogeneous, and we expect that, even when $t/\delta\epsilon$ does not reach the critical value, we can also obtain super-Poissonian noise by applying an inhomogeneous magnetic flux. To verify it we plot in figure 4(b) the variation of F with ϕ, where the parameters are the same as those in figure 4(a) except for $t/\delta\epsilon = 0.35$. Since the critical value of $t/\delta\epsilon$ is 0.354 in region 2, the shot noise is always sub-Poissonian if the flux is homogeneous. However, when the flux is inhomogeneous, super-Poissonian noise appears in this region again when $\theta + \phi \approx 2\pi$ and $|\phi - \theta| > \pi$, as revealed in this figure. This can be understood by the following considerations. If $\theta = 0$, the Fano factor reaches its maximum when $\phi = 0$ (or $\phi = 2\pi$). Now $\Gamma_1^L = \Gamma_1^R = \Gamma(1 - \sin 2\beta) < \Gamma_2^L = \Gamma_2^R = \Gamma(1 + \sin 2\beta)$ and the weakly coupled antibonding state enhances the bunching of tunneling events through the bonding state. When $\theta \neq 0$ and $\theta + \phi = 2\pi$, we have $\Gamma_1^L = \Gamma(1 + \sin 2\beta \cos\theta)$, $\Gamma_1^R = \Gamma(1 + \sin 2\beta)$, $\Gamma_2^L = \Gamma(1 - \sin 2\beta \cos\theta)$ and $\Gamma_2^R = \Gamma(1 - \sin 2\beta)$. Since in region 2 the transport properties are not affected by the interchange of the roles of the bonding and antibonding states, the system is equivalent to the one with coupling strengths $\Gamma_1^L = \Gamma(1 - \sin 2\beta \cos\theta)$, $\Gamma_1^R = \Gamma(1 - \sin 2\beta)$, $\Gamma_2^L = \Gamma(1 + \sin 2\beta \cos\theta)$ and $\Gamma_2^R = \Gamma(1 + \sin 2\beta)$. Compared with the case $\theta = 0$, Γ_1^R and Γ_2^R are not changed. When θ increases from 0 to π, Γ_1^L increases while Γ_2^L decreases, which enhances the probability that the electrons reside in the antibonding state. Thus, the bunching of transport through the bonding state is further enhanced. When θ is small, the Fano factor is also enhanced, but when θ is large, F begins to decrease with θ, because now Γ_2^L is small and the current through the bonding state is much smaller than that when θ is small. In particular, when $\theta = \pi$, the shot noise is sub-Poissonian, which has

already been studied by us. So for a fixed $t/\delta\epsilon$, F should reach its maximum when $\theta+\phi\approx 2\pi$ and θ equals a certain value in the region $(0,\pi)$ (or $(\pi,2\pi)$). This can be clearly seen in figure 4(d), where $t/\delta\epsilon=0.35$, and other parameters are the same as those in figure 4(c). The maximum happens when $\theta+\phi\approx 2\pi$ and $|\phi-\theta|>\pi$. To obtain the analytical results we turn to equation (2). Substituting the expressions of the coupling strengths into this formula, we obtain

$$\begin{aligned}F=&\left\{\left[5+\sin^2 2\beta\cos\frac{\phi+\theta}{2}\right.\right.\\&\left.\left(\cos\frac{\phi+\theta}{2}+2\cos\frac{\phi-\theta}{2}\right)\right]\\&\times\left[1+\sin^2 2\beta\cos\frac{\phi+\theta}{2}\right.\\&\left.\left.\times\left(\cos\frac{\phi+\theta}{2}-2\cos\frac{\phi-\theta}{2}\right)\right]\right\}\\&\times\left\{\left[3-\sin^2 2\beta\cos\frac{\phi+\theta}{2}\right.\right.\\&\left.\left.\times\left(\cos\frac{\phi+\theta}{2}+2\cos\frac{\phi-\theta}{2}\right)\right]^2\right\}^{-1}.\end{aligned}\tag{3}$$

Then we can find for a fixed $t/\delta\epsilon$ that F reaches its maximal value $F_{\max}=(16-8\cos^2 2\beta+\cos^4 2\beta)/(16\cos^2 2\beta)$ when $\theta+\phi=2\pi$ (or $\Phi_{\mathrm{R}}=\Phi_0/2$) and $|\phi-\theta|=2\cos^{-1}[(1-\sin^4 2\beta-8\sin^2 2\beta)/(10\sin^2 2\beta-2\sin^4 2\beta)]$, which is consistent with our previous analysis. For $t/\delta\epsilon=0.35$, $F_{\max}\approx 1.032$ when $\phi\approx 1.691\pi$ and $\theta\approx 0.309\pi$ (or $\phi\approx 0.309\pi$ and $\theta\approx 1.691\pi$). By assuming $F_{\max}=1$, we find the reduced critical value $t/\delta\epsilon\approx 0.338$. So we see again that the inhomogeneous distribution of the magnetic flux makes the generation of the super-Poissonian noise easier. The corresponding behaviors of the shot noise in region 3 are similar, so we do not discuss them here anymore.

In some of the previous studies on the similar structure, it has been pointed out that the conductance is a periodic function of ϕ with period 4π [32, 40, 41], since the conductance depends on the coupling strengths, and when ϕ changes 4π, the coupling strengths return to their original values. This is valid if ϕ and θ varies independently. However, if $\phi/\theta=(n+1)/(n-1)$ (or $\Phi_{\mathrm{R}}/\Phi_{\mathrm{L}}=n$) is kept, the period changes to $2(n+1)\pi$ [32, 41]. The Fano factor is also determined by the coupling strengths and the transport regimes, so we expect to observe similar oscillations of the Fano factor. In figures 5(a) and (b) we show the oscillations of the Fano factor in regions 2 and 3, respectively. In figure 5(a) we see that, for different values of ϕ/θ, the shot noise can be enhanced to super-Poissonian noise for different times in one period. This can also be seen in figure 4(c). Besides, for $\phi/\theta=1, 0.5$ and 2, the periods should be 2π, 4π and 8π, respectively, while in figure 5(a), different from our expectation, the periods are 2π, 2π and 4π. The reason is that in region 2 the shot noise is not affected by the interchange of the role of the bonding and antibonding states. For $\phi/\theta=0.5$, when $\phi=2\pi$, the values of Γ_1^α and Γ_2^α just interchange, so the Fano factor remains unchanged. In region 3 this symmetry does not hold, so we can observe in figure 5(b) the expected oscillations of the Fano factor with periods 2π, 4π and 8π.

In our previous calculations we always assume $U>\epsilon_1-\epsilon_2$, so the double occupation is forbidden for a low bias. Here we briefly examine the case $U<\epsilon_1-\epsilon_2$, and only consider the homogeneous distribution of the magnetic flux. In figure 5(c) the Fano factor as a function of the bias voltage for different ϕ is shown and the corresponding situation for the current is shown in the inset. Now there are only three steps in the I–V or $F-V$ curves located at ϵ_1, ϵ_2 and ϵ_2+U. As ϕ increases, Γ_1 increases, accompanied by the decrease of Γ_2, and I decreases in both regions, which is similar to the case when $U>\epsilon_1-\epsilon_2$. This is because, for $\epsilon_1<\mu_{\mathrm{L}}<\epsilon_2$, only the bonding state contributes to the current, and for $\epsilon_2<\mu_{\mathrm{L}}<\epsilon_2+U$ the decrease of Γ_2 enhances the blockade of transport through the antibonding state. The behavior of the shot noise is quite different from the case when $U>\epsilon_1-\epsilon_2$. If the magnetic flux is absent, we cannot generate super-Poissonian noise by increasing the interdot coupling strength, because now $\Gamma_2>\Gamma_1$ and the transport through the bonding state cannot be blocked by the electrons in the antibonding state. When the magnetic flux increases, Γ_1 increases while Γ_2 decreases, and finally leads to the blockade of transport through the antibonding state. Thus, when ϕ approaches π, super-Poissonian noise appears for $\epsilon_2<\mu_{\mathrm{L}}<\epsilon_2+U$, as revealed in figure 5(c). So we conclude that, even when $U<\epsilon_1-\epsilon_2$, we can still obtain super-Poissonian noise in the symmetrical system by the interplay between the interdot coupling and the magnetic flux.

We have carefully studied how super-Poissonian noise can be generated in the symmetrical system via the interdot coupling (or the interplay between the interdot coupling and the magnetic flux). At last we simply demonstrate the effect of the interdot coupling in an asymmetrical system, where the two dots have different coupling strengths to the leads. Dot a is assumed to be more strongly coupled to the leads, i.e. $\Gamma_a>\Gamma_b$. According to our previous discussions, the shot noise can be enhanced to be super-Poissonian in regions 2 and 3 for large enough Γ_a/Γ_b. If the interdot coupling is considered, it is expected that the noise will be suppressed, since the interdot coupling makes it possible that an electron trapped in dot b can tunnel to dot a and then to the lead, and consequently reduces the blockade. This has been pointed out by Djuric *et al* [25], where the spin-flip scattering plays the similar role to the interdot coupling in the present work. However, in their work the strength of the spin-flip scattering must be very small. As we have stated before, when the strength of the interdot coupling is large, it can result in some other effects, such as the level splitting and the renormalization of the coupling strengths. So it is necessary to check if the interdot coupling has other effects on the shot noise in the asymmetrical system. Here we would like to give some analysis before presenting the numerical results. After performing the same unitary transformation, the coupling strengths of the antibonding and bonding states are obtained as $\Gamma_1=\Gamma_a\cos^2\beta+\Gamma_b\sin^2\beta-\sqrt{\Gamma_a\Gamma_b}\sin 2\beta$ and $\Gamma_2=\Gamma_a\sin^2\beta+\Gamma_b\cos^2\beta+\sqrt{\Gamma_a\Gamma_b}\sin 2\beta$. To simplify the two expressions we define $\sin\varphi=\sqrt{\Gamma_a}/\sqrt{\Gamma_a+\Gamma_b}$ and $\cos\varphi=\sqrt{\Gamma_b}/\sqrt{\Gamma_a+\Gamma_b}$. Clearly $\pi/4<\varphi<\pi/2$, and $\Gamma_{1,2}$ can be expressed as $\Gamma_1=(\Gamma_a+\Gamma_b)\sin^2(\varphi-\beta)$ and

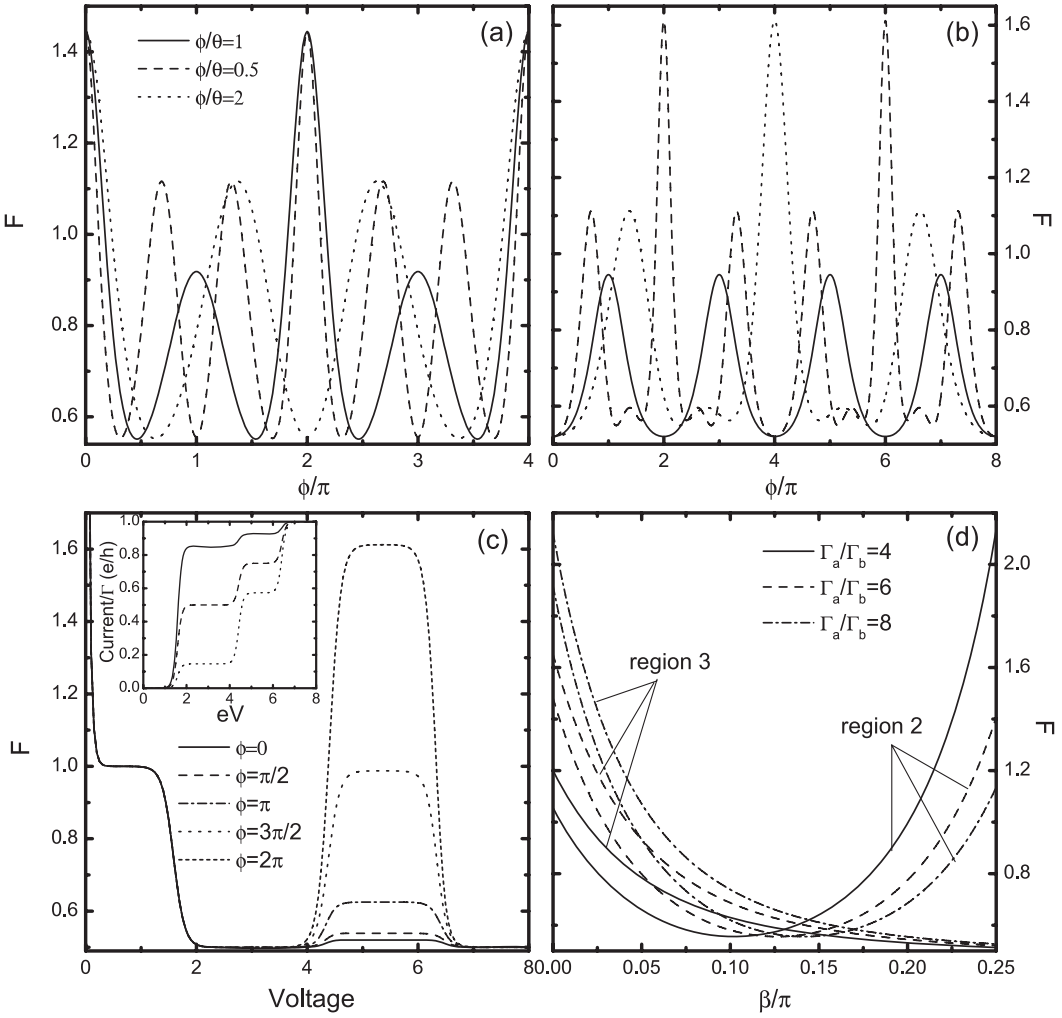

Figure 5. The flux dependence of the Fano factor in (a) region 2 and (b) region 3 for different values of ϕ/θ. $t/\delta\epsilon = 0.5$. In (c) we show the Fano factor versus bias voltage for $U < \epsilon_1 - \epsilon_2$. $\epsilon_a = 1$, $\epsilon_b = 2$, $t = 0.5$ and $U = 1$. The inset shows the corresponding situation for the current, where the solid, dashed and dotted lines corresponded to $\phi = 0$, π and 2π, respectively. The Fano factor as a function of β in asymmetrical systems is shown in (d).

$\Gamma_2 = (\Gamma_a + \Gamma_b)\cos^2(\varphi - \beta)$. Since $0 < \beta < \pi/4$, $\Gamma_1/\Gamma_2 = \tan^2(\varphi - \beta)$ decreases with β increasing. So in region 3 the Fano factor is always suppressed by the interdot coupling. The situation is different in region 2. With $t/\delta\epsilon$ increasing, Γ_1/Γ_2 decreases to 1 when $\varphi - \beta = \pi/4$. This can always be achieved, since $\pi/4 < \varphi < \pi/2$ and β can approach $\pi/4$ for large enough $t/\delta\epsilon$. In this process F keeps decreasing. For further increasing $t/\delta\epsilon$, Γ_1 is smaller than Γ_2 and the Fano factor begins to increases with $t/\delta\epsilon$. So in region 2 the Fano factor depends non-monotonically on $t/\delta\epsilon$. In figure 5(d) we plot the Fano factor in several asymmetrical systems as a function of β. As we expected, in region 3 the Fano factor decreases monotonically with β, while in region 2 the Fano factor first decreases and then increases with β. For large enough $t/\delta\epsilon$, the Fano factor can be even larger than its original value, i.e. $\cos(\varphi - \pi/4)/\sin(\varphi - \pi/4) > \sin\varphi/\cos\varphi$. This happens if $\varphi < 3\pi/8$ or $\Gamma_a/\Gamma_b < 5.828$. So in different transport regimes the interdot coupling has different effects on the shot noise in the asymmetrical system.

4. Summary

In summary, we have studied the effects of the interdot coupling and the magnetic flux in a symmetrical double QD system. The interdot coupling induces the renormalization of the coupling strengths between dots and leads, thus generating super-Poissonian noise in certain bias ranges. Since the coupling strengths are flux-dependent, the magnetic flux can be utilized to accurately tune the value of the shot noise and change the bias range where super-Poissonian noise appears. If the distribution of the magnetic flux is inhomogeneous, the shot noise can be reduced or further enhanced. In the asymmetrical system, the interdot coupling can enhance or suppress the shot noise, which depends on the bias range.

Acknowledgments

This project was supported by the National Natural Science Foundation of China (no. 10774083), the Specialized Research Fund for the Doctoral Program of Higher Education (no. 2006003047) and the 973 Program (no. 2006CB605105).

References

[1] Hershfield S 1992 *Phys. Rev.* B **46** 7061
[2] Ding G H and Ng T K 1997 *Phys. Rev.* B **56** 15521(R)
[3] Blanter Y M and Büttiker M 2000 *Phys. Rep.* **336** 1
[4] Jehl X, Sanquer M, Calemczuk R and Mailly D 2000 *Nature* **405** 50
[5] Kozhevnikov A A, Schoelkopf R J and Prober D E 2000 *Phys. Rev. Lett.* **84** 3398
[6] Picciotto R D, Reznikov M, Heiblum M, Umansky V, Bunin G and Mahalu D 1997 *Nature* **389** 162
[7] Saminadayar L, Glattli D C, Jin Y and Etienne B 1997 *Phys. Rev. Lett.* **79** 2526
[8] Onac E, Balestro F, Beveren L H W V, Hartmann U, Nazarov Y V and Kouwenhoven L P 2006 *Phys. Rev. Lett.* **96** 176601
[9] Onac E, Balestro F, Trauzettel B, Lodewijk C F J and Kouwenhoven L P 2006 *Phys. Rev. Lett.* **96** 026803
[10] Schottky W 1918 *Ann. Phys., Lpz.* **57** 541
[11] Büttiker M 1990 *Phys. Rev. Lett.* **65** 2901
[12] Korotkov A N 1994 *Phys. Rev.* B **49** 10381
[13] Chen L Y and Ting C S 1991 *Phys. Rev.* B **43** 4534
[14] Büttiker M 1991 *Physica* B **175** 199
[15] Iannaccone G, Lombardi G, Macucci M and Pellegrini B 1998 *Phys. Rev. Lett.* **80** 1054
[16] Kuznetsov V V, Mendez E E, Bruno J D and Pham J T 1998 *Phys. Rev.* B **58** 10159(R)
[17] Blanter Y M and Büttiker M 1999 *Phys. Rev.* B **59** 10217(R)
[18] Song W, Mendez E E, Kuznetsov V and Nielsen B 2003 *Appl. Phys. Lett.* **82** 1568
[19] Bułka B R 2000 *Phys. Rev.* B **62** 1186
[20] Kießlich G, Wacker A and Schöll E 2003 *Phys. Rev.* B **68** 125320
[21] Safonov S S, Savchenko A K, Bagrets D A, Jouravlev O N, Nazarov Y V, Linfield E H and Ritchie D A 2003 *Phys. Rev. Lett.* **91** 136801
[22] Thielmann A, Hettler M H, König J and Schön G 2005 *Phys. Rev.* B **71** 045341
[23] Belzig W 2005 *Phys. Rev.* B **71** 161301(R)
[24] Braun M, König J and Martinek J 2006 *Phys. Rev.* B **74** 075328
[25] Djuric I, Dong B and Cui H L 2006 *J. Appl. Phys.* **99** 063710
[26] Wela E, Oreg Y, Oppen F V and Koch J 2006 *Phys. Rev. Lett.* **97** 086601
[27] Sánchez R, Platero G and Brandes T 2007 *Phys. Rev. Lett.* **98** 146805
[28] Gattobigio M 2002 *Phys. Rev.* B **65** 115337
[29] Holleitner A W, Decker C R, Qin H, Eberl K and Blick R H 2001 *Phys. Rev. Lett.* **87** 256802
[30] Holleitner A W, Blick R H, Hüttel A K, Eberl K and Kotthaus J P 2002 *Science* **297** 70
[31] Lu H Z, Lü R and Zhu B F 2005 *Phys. Rev.* B **71** 235320
[32] Bai Z M, Yang M F and Chen Y C 2004 *J. Phys.: Condens. Matter* **16** 2053
[33] Liu Y S, Chen H and Yang X F 2007 *J. Phys.: Condens. Matter* **19** 246201
[34] Dong B, Cui H L and Lei X L 2004 *Phys. Rev.* B **69** 035324
[35] Thielmann A, Herrler M H, König J and Schön G 2003 *Phys. Rev.* B **68** 115105
[36] Guevara M L L D, Claro F and Orellana P A 2003 *Phys. Rev.* B **67** 195335
[37] Guevara M L L D and Orellana P A 2006 *Phys. Rev.* B **73** 205303
[38] Barthold P, Hohls F, Maire N, Pierz K and Haug R J 2006 *Phys. Rev. Lett.* **96** 246804
[39] Sánchez R, Kohler S, Hänggi P and Platero G 2008 *Phys. Rev.* B **77** 035409
[40] Kang K and Cho S Y 2003 *J. Phys.: Condens. Matter* **16** 117
[41] Jiang Z T, You J Q, Bian S B and Zheng H Z 2002 *Phys. Rev.* B **66** 205306